Methodology for the systematic investigation of the hygrothermal-mechanical behavior of a structural epoxy adhesive

S. Sander[a*], G. Meschut[a], U. Kroll[b], A. Matzenmiller[b]

[a]*Laboratory for Material and Joining Technology (LWF), Paderborn University, 33098 Paderborn, North Rhine-Westphalia, Germany*

[b]*Institute of Mechanics (IfM), University of Kassel, 34125 Kassel, Hessen, Germany*

*) Sascha Sander, Pohlweg 47-49, 33098 Paderborn, FON: +49 5251 60-5580, FAX: +49 5251 60- 3239, E-Mail: sascha.sander@lwf.upb.de

Methodology for the systematic investigation of the hygrothermal-mechanical behavior of a structural epoxy adhesive

Short Abstract

A methodology is presented for the systematic determination of moisture absorption behavior of a structural epoxy adhesive in order to investigate the influence of humidity on the strength, fracture energy and fracture strain of adhesively bonded joints subjected to monotonic quasi-static loading. The first step consists of a preliminary weighting test to assess the parameters of the Fick diffusion model for the adhesive at hand by means of a thin disc made of cured adhesive bulk material. Numerical simulations verify the applied assumption of one-dimensional diffusion. It turns out that the adhesive disc is not thin enough in order to achieve reasonable testing times up to saturation for the complete characterization of moisture absorption. Therefore, the specimen thickness is systematically reduced.

In the second step, the diffusion behavior of the adhesive is characterized. In order to get a homogeneous humidity level within the whole specimen, several adhesive discs are exposed to a reference temperature and humidity, according to the prior dimensioning. This novel procedure of preconditioning allows for a homogeneous and, thus, well-defined initial state of water content in the specimens. From this state, the discs are exposed to various environmental conditions, which include different temperatures and relative humidity of the surrounding moist air. It is observed that moisture saturation primarily depends on the relative humidity, while the diffusion coefficient depends on temperature for this epoxy adhesive. Fick's model of diffusion is applied to represent the moisture uptake of the adhesive at hand, whereby the initial state of water saturation after preconditioning is taken into account.

Based on the findings in step 1 and 2, the influence of moisture is determined in step 3 on the strength, fracture energy and elongation at rupture of adhesively bonded joints. Thick

adherend shear specimens (TASSs) are preconditioned in order to achieve a variety of homogeneous moisture states in the corresponding adhesive layer. After preconditioning, quasi-static tensile tests of the TASSs are carried out at various temperature levels. The experimental results reveal that the strength and fracture energy of the TASS degrades progressively with higher temperature and increased humidity.

Introduction

Structural adhesives are so-called tough modified epoxy polymers. Typical structural adhesives like the investigated one component, hot curing Betamate^{TM} 1496V by DuPont de Nemours consist of a brittle matrix of epoxy-resin, in which elastomeric particles are embedded by chemical bonds [1]. These particles with a diameter of a few micrometers act as tougheners and increase the ductility of the material compound under mechanical loading, as they reduce local stress concentrations and delay the growth of micro cracks due to damage [2]. This compound results in a high energy absorption for crash loading and improvement of the lifetime due to cyclic mechanical loads [3].

The numerous advantages of structural adhesives are limited by the environmental conditions on the lifetime of the adhesive layer, since these mixtures show hygroscopic behavior in water and moist air, which is known to be accelerated by the temperature [4]. The hygrothermal loading successively reduces the lifetime of the adhesive joint by hydrolysis, deteriorating the integrity of the polymer network [5]. This process needs to be predicted in order to guarantee the long-term structural integrity during the service in order to avoid fatal failure of bonded components. The first steps, therefore, include the characterization and modeling of the water absorption behavior for the adhesive.

There are a variety of approaches to model diffusion in an adhesive. The simplest and most common one is the Fick assumption [6]. Although the single Fickian sorption is the most common type of water diffusion model for adhesives, however, other types of behavior also

exist [7] [8]. These anomalous properties are often described by using a dual Fickian model. The data for this model is usually determined by gravimetric experiments [9]. Samples are stored in water or moisture in accordance with DIN EN ISO 62:2008 and weighed at regular intervals. The diffusion coefficient is determined by the rate of weight increase of the adhesive. Usually, the samples are first completely dried at higher temperature levels (DIN EN ISO 62:2008). This can lead also in other components in addition to water resorption out of the adhesive.

In this study, a methodology is presented, to determine the parameters for the water adsorption at an initial defined water concentration making additional drying down to zero percent relative humidity (RH) unnecessary. The water adsorption up to saturation is used to subsequently characterize the adhesive behavior of differently saturated bonded specimens. The mechanical testing is usually investigated only at 22.5 °C – 50% RH, but with an undefined moisture content within the adhesive layer – see DIN EN 14869-2 or DIN EN ISO 527- 2.

Water sorption of structural adhesives

Water absorption of the structural adhesive is governed by several mechanisms of diffusion [10], [11], [12]. Water molecules can penetrate into the adhesive through the epoxy matrix and accumulate at cracks or cavities. A second diffusion mechanism is the water accumulation at the interfaces between the tougheners and the matrix. Another mechanism is the diffusion through the interface between the adhesive and the adherends. Each diffusion mechanism may be investigated and modeled individually. However, in the following, no distinction is made between the diffusion mechanisms. Water diffusion will be investigated as a whole.
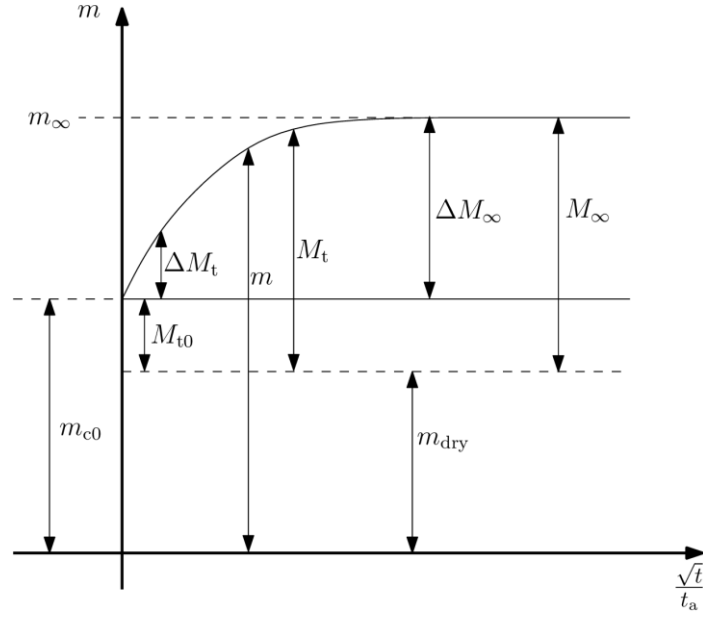
Figure 1: Sketch of weight increase due to moisture diffusion

Water diffusion leads to moisture uptake in the structural adhesive, resulting in weight increase. The characteristic variables for this process are illustrated in Figure 1 for a thin hygroscopic bulk material with thickness t_a, which is small compared to the remaining dimensions. If a thin specimen of such material with mass m_{dry} is dry and exposed to wet air with relative humidity $\varphi_1 > 0$, then the mass of the specimen increases by the mass of water M_{t0} until saturation, where the value m_{c0} is attained. The mass of water in the specimen for this initial state of saturation is:

$$M_{t0} = m_{c0} - m_{dry} \tag{1}$$

From this initial state of saturation, the specimen may be exposed next to the higher relative humidity $\varphi_2 > \varphi_1$. For the moisture diffusion of this process, the solid line in Figure 1 represents the actual mass m over the quotient of the square root of time t and t_a. The actual mass of water in the specimen is

$$M_t = m - m_{dry} \tag{2}$$

and the mass of water at saturation is denoted by

$$M_\infty = m_\infty - m_{\text{dry}} = V c_\infty \,, \tag{3}$$

where m_∞, V and c_∞ denote the mass of the specimen at saturation, the actual volume of the specimen and the water concentration in the specimen at saturation. The increase in volume due to water uptake is neglected for simplicity.

As a result, the mass of increase of water from the initial to the actual state is given by:

$$\Delta M_{\text{t}} = M_{\text{t}} - M_{\text{t0}} \tag{4}$$

The mass of increase of water from initial state up to saturation is:

$$\Delta M_\infty = M_\infty - M_{\text{t0}} = m - m_{\text{c0}} \tag{5}$$

The measurement of the specimen's weight over time allows for an indirect determination of diffusion by means of a diffusion model as outlined next.

Diffusion model

The governing equations are presented for the theory of Fick's diffusion in the following [13]. According to this approach, the diffusion is represented by the linear diffusion differential equation with a constant scalar diffusion coefficient. Then, the diffusion behavior of the material is denoted as homogeneous [6], [14]. The solution of this diffusion model results for the one-dimensional case in the following concentration c along the coordinate x in a thin structure with thickness t_{a} over time t [6]:

$$\frac{c - c_{\text{t0}}}{c_\infty - c_{\text{t0}}} = 1 - \frac{4}{\pi} \sum_{i=0}^{\infty} \frac{(-1)^i}{2i + 1} \exp\left(-\frac{D(2i + 1)^2 \pi^2 t}{t_{\text{a}}^2}\right) \cos\frac{(2i + 1)\pi x}{t_{\text{a}}} \tag{6}$$

In equation (6), c_{t0} and c_∞ denote the initial concentration at time $t = 0$ and the final concentration at complete saturation. The material parameter D is the diffusion coefficient. The ratio of the actual water uptake with respect to the total one at saturation results from the integration of equation (6) through the thickness, which yields:

$$\frac{\Delta M_{\text{t}}}{\Delta M_{\infty}} = \frac{M_{\text{t}} - M_{\text{t0}}}{M_{\infty} - M_{\text{t0}}} = 1 - \frac{8}{\pi^2} \sum_{i=0}^{\infty} \frac{\exp\left(-\frac{D(2i+1)^2\pi^2 t}{t_{\text{a}}^2}\right)}{(2i+1)^2} \tag{7}$$

For short time intervals of diffusion, equation (7) becomes

$$\frac{M_{\text{t}} - M_{\text{t0}}}{M_{\infty} - M_{\text{t0}}} = 4\sqrt{\frac{D}{\pi}} \frac{\sqrt{t}}{t_{\text{a}}}, \tag{8}$$

cf. [6]. The diffusion coefficient apparently determines the slope of a straight line in equation (8), where the left hand side and $\sqrt{t}/t_{\text{a}}$ on the right hand side are the dependent and independent variables. Inserting equations (1), (2), and (3) into equation (8) leads to:

$$\frac{m - m_{\text{c0}}}{m_{\infty} - m_{\text{c0}}} = 4\sqrt{\frac{D}{\pi}} \frac{\sqrt{t}}{t_{\text{a}}} \tag{9}$$

The dependence of the diffusion coefficient on the temperature T is considered by the ARRHENIUS-type equation in [11]:

$$D = D_0 \exp\left[D_1\left(\frac{1}{T_{\text{ref}}} - \frac{1}{T}\right)\right], \tag{10}$$

where T_{ref} is a reference temperature and D_0, D_1 are constitutive parameters. Furthermore, the dependence of the water uptake at saturation on the relative humidity φ is considered by the approach in [12]:

$$M_{\text{max}} = a\varphi^b = \frac{M_{\infty}}{m_{\text{dry}}} \quad , \quad M_{\infty} = m_{\text{dry}}a\varphi^b = \tilde{a}\varphi^b \tag{11}$$

In equation (11), the relative humidity (RH) of the surrounding wet air is given in percent and $a, b, \tilde{a}$ are parameters, which depend on the hygroscopic behavior of the material at hand. Equations (5) and (11) yield:

$$\Delta M_{\infty} = \tilde{a}\varphi^b - M_{\text{t0}} \tag{12}$$

Therefore, the water concentration is given at saturation with respect to the initial state by:

$$\Delta c_\infty = \frac{\Delta M_\infty}{V} = \frac{\tilde{a}\varphi^b - M_{t0}}{V} \tag{13}$$

Experimental setup and dimensioning of the disc geometry

For a preliminary investigation, a gravimetric test is carried out on a thin adhesive disc, as illustrated in Figure 2. First, the adhesive is applied between two steel plates, covered with polytetrafluoroethylene (PTFE). The plates are placed in a preheated press. Pressure is applied and the adhesive is cured at 180 °C for 30 minutes. The adhesive thickness t_a of the bulk material is kept at 1.5 mm with steel spacers. An adhesive disc with a diameter of $d = 30$ mm is then punched from the adhesive bulk material. Finally, the edges are sanded smooth with a fine sandpaper and care was taken to ensure that the specimens had no imperfections (e.g. air bubbles) and are as homogeneous as possible.
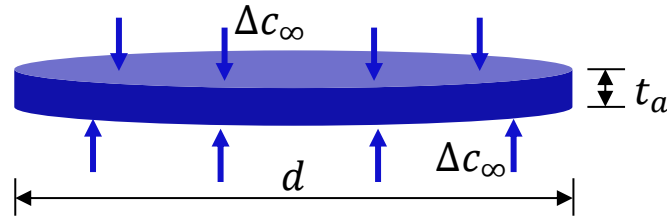

Figure 2: Geometry of adhesive disc with diameter 30 mm *and thickness* 1.5 mm

The sample is then aged in a climatic test chamber (CTS C -40/600, with a sensitivity of temperature of ± 0,3 and humidity of ± 1,5) at a temperature level of $\vartheta = 22.5$ °C and 80% relative humidity RH. During that time, the mass m is measured with a precision balance (Mettler Toledo XS205 DualRange, with a sensitivity of 0.01 mg) at specified time intervals. For this purpose, the samples are taken from the climatic chamber, weighted and put back into storage.
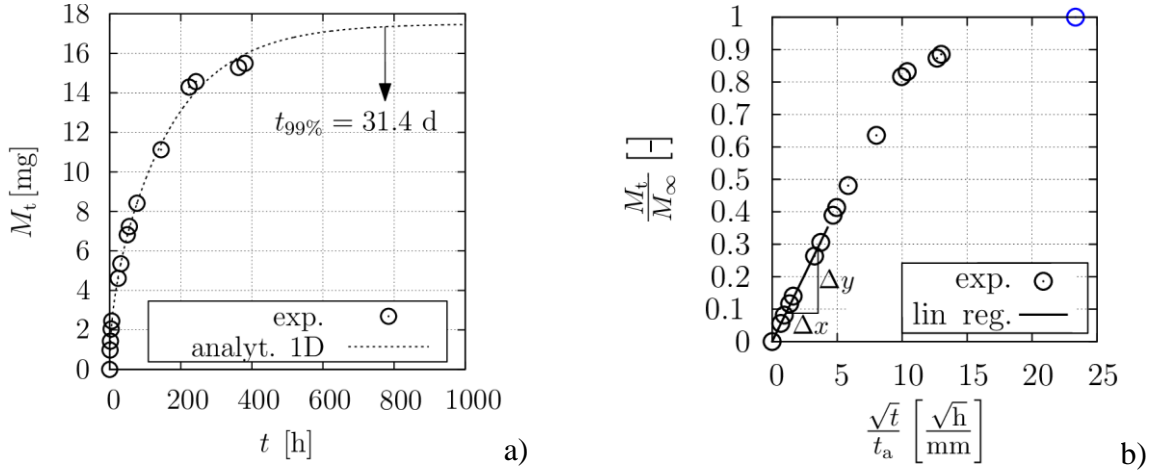
Figure 3: Moisture absorption of adhesive disc with thickness 1.5 mm *at 22.5 °C and 80% RH; a) mass change and b) relative mass change*

The results of the preliminary investigations are illustrated in Figure 3, where the measured weight is denoted by "exp.". A dry specimen at test start is assumed, i. e. $M_{t0} = 0$. Furthermore, the test data point for saturation at $\Delta M_\infty = M_\infty = 17.5$ mg (blue) has been cautiously assumed.

The thickness of the adhesive disc is small compared to its diameter, so the disc represents a thin structure, for which the theory of one-dimensional diffusion holds in good agreement. Consequently, the Fick coefficient of diffusion may be identified by the slope $\Delta y / \Delta x$, which is a result of the linear regression (lin. reg.) through the first seven data points in Figure 3. As a result, the slope yields the following value for the diffusion coefficient according to equation (8):

$$D = 3.696 \cdot 10^{-7} \text{ mm}^2/\text{s} \tag{14}$$

This value corresponds well to the order of magnitude of typical diffusion coefficients of epoxy resins, see [2] and [15]. The one-dimensional Fick diffusion model together with the assumption of a dry specimen at test start yields equation (7) with $M_{t0} = 0$, which is illustrated in Figure 3 (left, dashed line), where the value of the diffusion coefficient in equation (14) is used for plotting. Figure 3 (left) shows that 99% of water uptake at saturation is reached after a

little more than 30 days, which is too long for a practical characterization of the diffusion behavior. Therefore, the specimen geometry is adjusted.
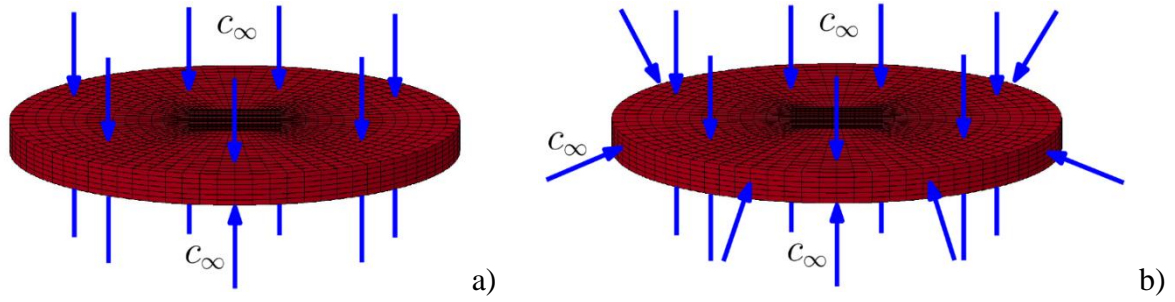

Figure 4: FE-models for three-dimensional diffusion with a) one- and b) two-dimensional boundary assumption

For this purpose, FE-simulations of the diffusion process are performed with the commercial software LS-DYNA [16], for the FE-models in Figure 4, illustrating the FE-meshes of the adhesive disc with thickness $t_{\mathrm{a}} = 1.5$ mm as in Figure 2 for two different three-dimensional computations. The FE-models in Figure 4 a) and b) differ with respect to the boundary assumption for diffusion. In the case of Figure 4 a), diffusion only takes place in thickness direction normal to the specimen. Therefore, this FE-model corresponds to a one-dimensional diffusion model, see Figure 5 a). In the other case of Figure 4 b), radial diffusion along the circumferential direction is considered in addition, which is why this FE-model corresponds to two-dimensional diffusion, see Figure 5 b). The boundary condition for the diffusion problem consists of a prescribed concentration $\Delta c_{\infty} = c_{\infty} = M_{\infty}/V$, see equation (13), since a dry specimen is assumed, which means $M_{\mathrm{t0}} = 0$.

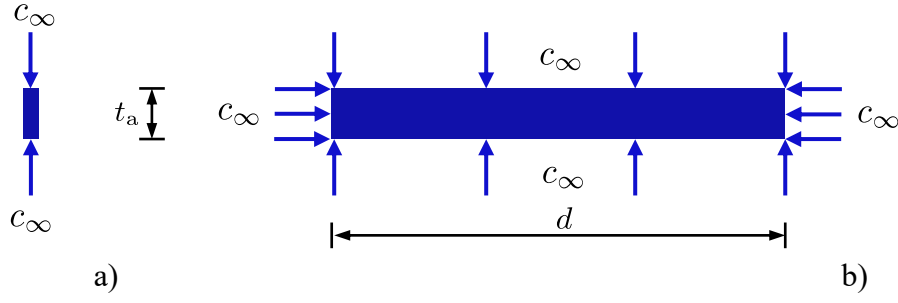a)   b)

Figure 5: Idealization of three-dimensional diffusion models in Figure 4 with boundary assumption for a) one- and b) two-dimensional diffusion process

The concentration boundary condition is applied to the corresponding nodes of the FE-models according to the one- and two-dimensional diffusion model. The diffusion problem is treated in LS-DYNA with the thermal solver, since the diffusion problem and the thermal one have analogous field equations and boundary conditions, see. e. g. [17] and [18] for a detailed description.

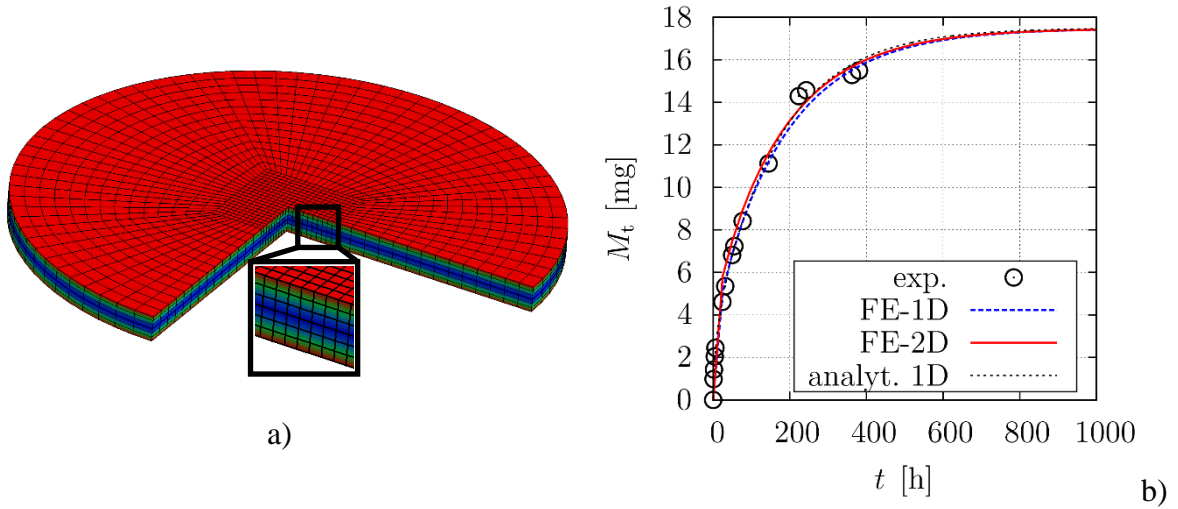a)   b)

Figure 6: a) Concentration in disc (high concentration in red, low concentration in blue) and b) analytical and numerical FE-solution for moisture uptake compared to test data as in Figure 3 a)

The simulation results for the one- and two-dimensional diffusion problem are denoted as "FE-1D" and "FE-2D" and compared to the analytical solution (analyt. 1D) as in equation (7), see Figure 6 b). The diffusion coefficient is used from equation (14). The coincidence of the simulations and the analytical solution in Figure 6 b) verifies the numerical solution and justifies

the idealization of the adhesive disc as a thin structure for the diffusion problem at hand. It shows that there is no significant difference between the 1D and 2D-diffusion model. In order to reduce the time until saturation for a specific material, the thickness of the specimen must be reduced according to equation (7).
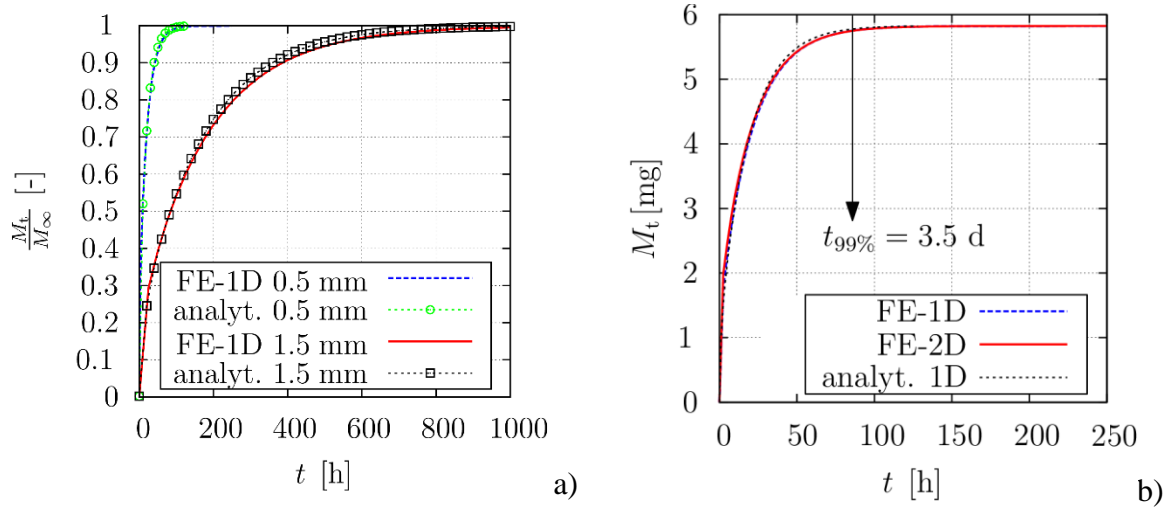

Figure 7: Comparison of FE-simulations (FE-1D, FE-2D) and analytical solutions (analyt.): a) one-dimensional diffusion model for thicknesses 0.5 mm *and* 1.5 mm *and b) one- and two-dimensional diffusion process for thickness* 0.5 mm

The mass increase over time [in hours] is compared for the one-dimensional FICKian diffusion approach up to saturation in Figure 7 (left), where two different thickness values are investigated. The analytical and numerical solution coincide for both thickness values in Figure 7 a). The time until saturation of 99%, which means $M_t/M_\infty = 0.99$, amounts to $t_{99\%} = 3.5$ d (days) for the thickness of $t_a = 0.5$ mm, see Figure 7 b). Thus, the disc thickness of $t_a = 0.5$ mm requires a test duration, which allows for a practical characterization of the diffusion behavior.
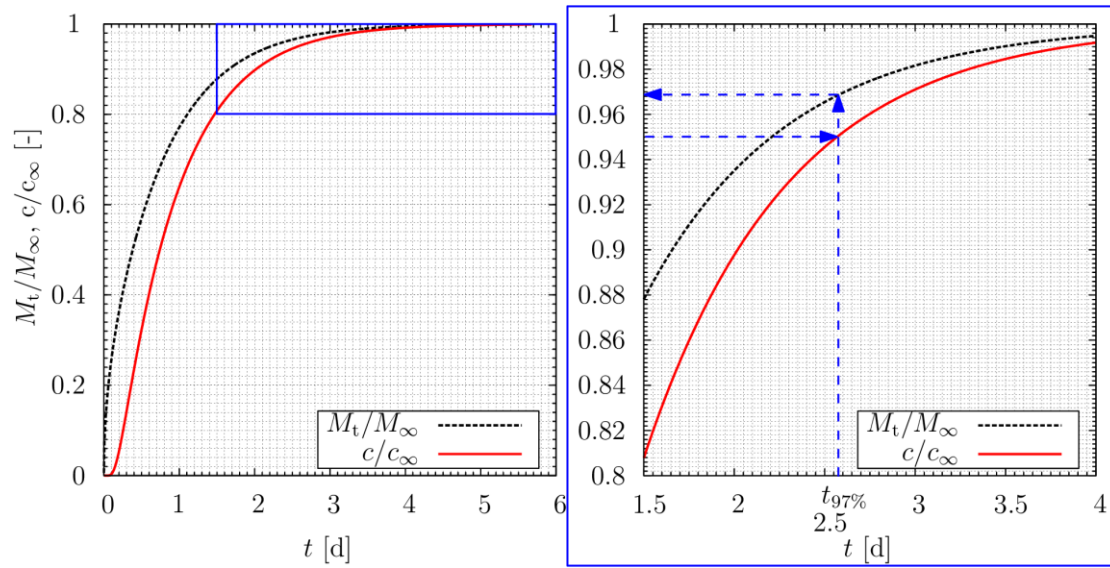
Figure 8: Relative water content and concentration versus time at the center of disc

In Figure 8, course of relative water content and concentration are depicted over time according to equation (7) and (6) at the center $x = 0$, where the diffusion coefficient as in equation (14) is used and a dry specimen is assumed for the initial state with $M_{t0} = c_{t0} = 0$. The result is summarized in the following conclusion: If the difference between the desired state of saturation according to equation (7) and the local concentration according to equation (6) in the center of the specimen at $x = 0$ should be no more than 5% for the one-dimensional diffusion problem, then one has to wait at least 97% of the time until complete saturation $t_{97\%} = 2.6$ d is reached. So the state of humidity is almost homogeneous in the specimen at this point of time. It should be noted that this is also the case in the previous investigations, where the time interval $t_{99\%} = 3.5$ d is needed for saturation.

Characterization of the diffusion behavior

Adhesive discs are produced with the same procedure as described above, but with a thickness of $t_a = 0.5$ mm and a diameter of $d = 40$ mm, in order to obtain durations of practical magnitude in the tests for water uptake until saturation. In order to achieve a constant water saturation of the samples prior to ageing, the samples are conditioned at 22.5 °C - 50% RH until no more weight change can be detected in three successive measurements,

according to DIN EN ISO 62:2008-05. Afterwards, the samples are weighed to determine m_{c0} and aged in a climatic test chamber with the parameters as given in Table 1. Three samples are tested simultaneously in each chamber. The weight of the specimens is detected during ageing with the same scale and procedure as for the previous tests.

Table 1: Test parameters: temperature ϑ and relative humidity φ

ϑ [°C]	22.5	40	70
φ [%]	/	5	5
	50	50	50
	80	80	80

The saturation and diffusion properties of the structural adhesive are determined on the basis of experimental methods described. Figure 9 shows the experimental results of the different ageing tests. It can be seen that the mass increase is faster at higher temperature, especially in the initial phase of diffusion. At the beginning of the test, the diffusion is linear with the square root of time. After that, the water uptake is delayed and asymptotically approaches the state of saturation as expected.

The experiments also show that the saturated samples, subjected to a very dry environment, at 40 °C - 5% RH as well as at 70 ° - 5% RH, have released almost the same amount of absorbed water in both cases. This observation suggests that the maximum moisture absorption is independent of the temperature level. This hypothesis is confirmed by the results of the exposed samples at 80% RH and 50% RH with three different temperature levels: also almost the same amount of water is absorbed in all three cases. The slight increase at 40 °C - 50% RH is most likely due to the measuring accuracy of the process. In contrast to further investigations [19], the speed of diffusion is the same for adsorption and resorption.
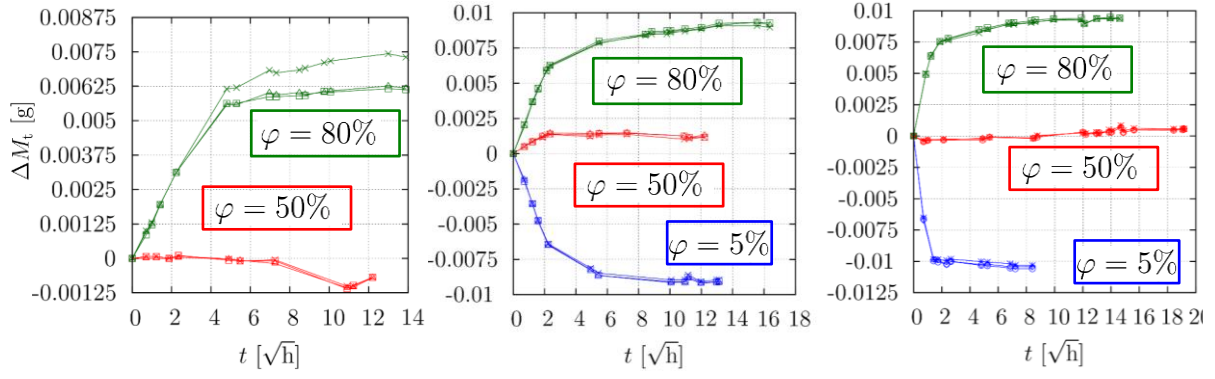
Figure 9: Moisture absorption of adhesive sample with thickness 0.5 mm *at* 22.5 °C *(left),*

40 °C (middle) and 70 °C (right) and three different relative humidities φ

Out of these experimental results, the diffusion coefficient and the moisture saturation can

now be derived. As s shown in Figure 10, the diffusion coefficient can be determined from the

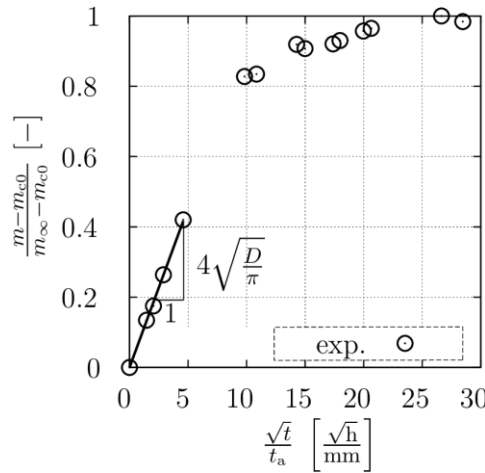initial slope of the saturation curve by using equation (9).

Figure 10: Example for determination of diffusion coefficient at 22.5 °C - 80% RH

The mass at saturation is determined as followed from the test data:

$$m_\infty = \max m\,(t) \tag{15}$$

The diffusion coefficients are determined for each parameter combination in Table 1 and the

result is shown in Figure 11 (left). The increase of the water mass ΔM_∞ from the initial state

up to saturation is plotted in Figure 11 (right). The parameters for the temperature-dependent

diffusion coefficient as in equation (10) and for the mass increase of water at saturation

according to equation (12) are computed by means of the least square method. Both results are shown in Figure 11. The identified parameters are listed in Table 2.
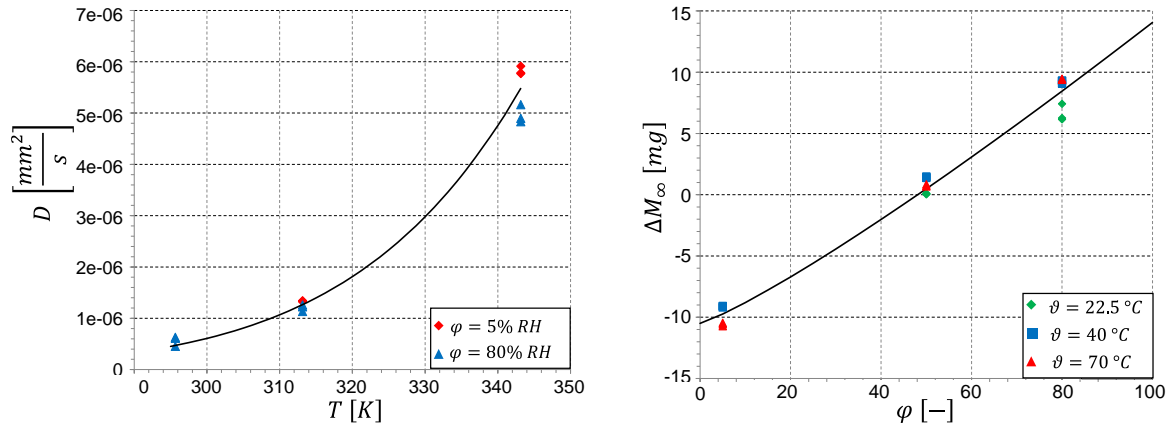

Figure 11: a) Test data and course of diffusion coefficient versus temperature as in equation (10) and b) mass increase for moisture saturation versus relative humidity according to equation (12)

Table 2: Identified parameters

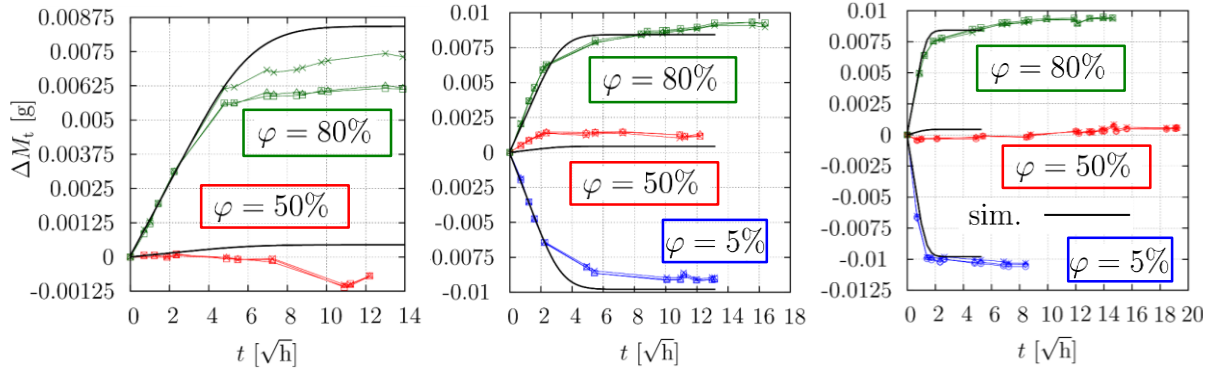| D_0 [mm²/s]	D_1 [K]	$\tilde{a}$ [mg]	b [-]	M_{t0} [mg]	T_{ref} [K]
$7.58 \cdot 10^{-6}$	6543.47	0.117	1.16104	10.5	343.15

Figure 12: Mass increase versus time of adhesive specimen for three different temperature levels at 22.5 °C (left), 40 °C (middle) and 70 °C (right): as measured in tests see Figure 9 and predicted by equation (7) *(black line)*

The water uptake is predicted with the parameters in Table 2 and equations (7), (10) and (12) and compared to the test data in Figure 12. No final conclusion can be made for the humidity of $\varphi = 50\%$, since the specimens ought to be saturated. For $\varphi = 5\%$ and $\varphi = 80\%$, the predictions of water uptake for short time intervals coincide very well with the test data, which proves the validity of the approach for the determination of the diffusion coefficient. At the point of transition to saturation, however, the water uptake is overestimated at $\varphi = 80\%$ for all temperatures and in the case at $\varphi = 5\%$ for $\vartheta = 40\,°C$. Overall, the prediction is in close agreement with the test data and suitable for a conservative component design.

Influence of temperature and moisture on bonded joints

The bonding characteristics of adhesives are strongly dependent on the environmental factor especially temperature and moisture. Therefore, the influence of hygro-thermal-mechanical (htm) loading on ageing resistance is analyzed for adhesively bonded steel joints. The adhesive layer are saturated under different climatic conditions in order to achieve a homogeneous saturation. Quasi-static tensile tests are carried out on different saturated adhesively bonded steel joints. Most adhesive joints in practice take very long time up to saturation. One possible technique to reduce the saturation time in experiments is to change the dimensions of the adhesive layer [20], [21].

Experimental setup and dimensioning of bonded joints

To characterize the mechanical joint properties, thick adherends shear specimens (TASS) according to DIN 14869-2 made of S235JR+AR steel are used. Based on the findings of the moisture diffusion behavior in the previous chapters, normalized TASS with an adhesive layer of 20x5 mm^2 have a too long timespan until moisture saturation is achieved, so the overlap length has to be reduced in these investigations. A suitable overlap length is identified by means of equation (16), which represents the two-dimensional extension of equation (7).

$$\frac{M_t}{M_\infty} = 1 - \frac{8}{\pi^2} \sum_{i=0}^{\infty} \sum_{j=0}^{\infty} \frac{\exp\left(-\frac{D(2i+1)^2\pi^2 t}{w_a^2}\right)}{(2i+1)^2} \frac{\exp\left(-\frac{D(2j+1)^2\pi^2 t}{l_0^2}\right)}{(2j+1)^2} \tag{16}$$

The overlap length is denoted by l_0 and the length of the adhesive layer by w_a. The course of mass increase versus time according to equation (16) is illustrated in Figure 13 for different temperatures and overlap lengths and a constant value of the width $w_a = 20\ mm$.
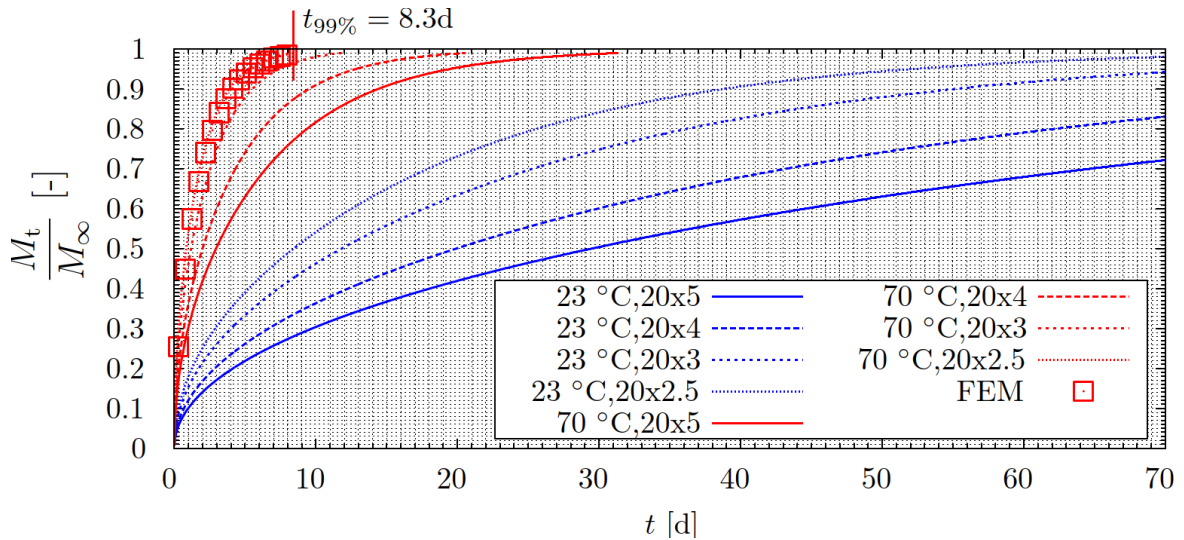

Figure 13: Computation of relative mass due to diffusion for different adhesive layer geometries (width x overlap length) for the shear specimen at 23 °C and 70 °C according to eg. (16) dotted and solid lines and FE simulation (FEM) of model in Figure 14 (squares).

With the smallest practical overlap length (from a manufacturing perspective) of 2.5 mm, it takes >70 days for the specimen to reach 99% saturation at 23 °C. This is too long for a practical

characterization of the mechanical behavior in a test . Therefore, a saturation temperature of 70 °C is used together with the adhesive layer dimension of the TASS with width $w_a = 20\ mm$ and length $l_0 = 2.5\ mm$ of layer. The selected temperature is lower than the glass transition temperature T_g of the adhesive (95-100 °C), to ensure that only physical processes take place and no chemical changes occur to the materials [22]. For 70 °C and $l_0 = 2.5\ mm$, Figure 13 additionally shows the coincidence with the FE solution due to the model in Figure 14. The application-typical adhesive layer thickness of $t_a = 0.3\ mm$ is adjusted with a special joining device.
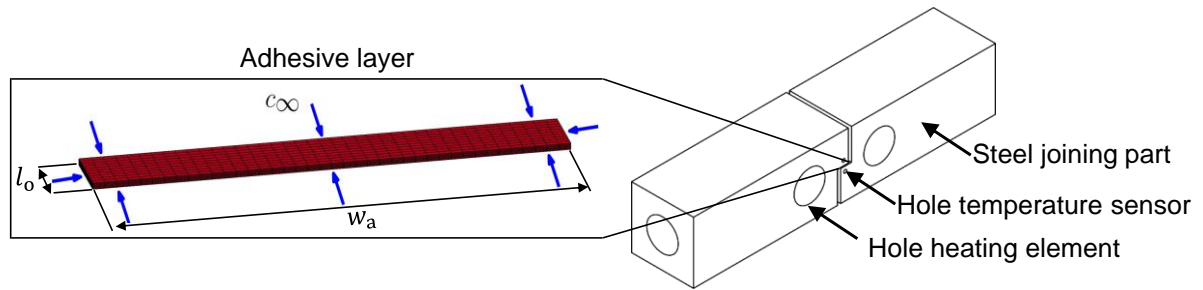

Figure 14: Geometry of TASS (right) and FE-Modell of adhesive layer in shear specimen (left)

Other studies show that surface pretreatment is of great importance for the failure mechanism of metallic adhesive joints under moist environment [22]. Therefore, the bonding surface is cleaned with acetone and sandblasted. To avoid corrosion and to achieve cohesive fracture behavior within the adhesive layer, it is then coated with the adhesion promoter DELO®-SACO PLUS. The SACO process (SAndblast COating process) offers high resistance to moisture, temperature and aggressive media. After joining the samples are cured in an oven at 180 °C for 30 minutes and afterwards stored in a climate chamber at 70 °C and different humidity levels in order to achieve a homogeneous moisture content within the adhesive layer.

The characterization of the investigated adhesively bonded joints under single quasi-static loading is carried out on a universal testing machine at a constant principal strain rate of 0.002 s^{-1}. The elongation is measured locally at the adhesive layer with an extensometer. The

tests are carried out at different temperatures, each with ≥ 3 repeats. Temperature- and moisture-dependent stress-strain curves are generated from the obtained data.

The shear stress τ is the quotient of the force F relative to the adhesive surface A, which can be calculated from the adhesive layer width w_a and overlap length l_o. The shear strain γ is determined by the quotient of the displacement Δu and the adhesive thickness t_a.

$$\tau = \frac{F}{A} \; = \; \frac{F}{w_a \cdot l_o} \; \left[\frac{N}{mm^2}\right] \tag{17}$$

$$\gamma = \arctan\left(\frac{\Delta u}{t_a}\right) \; [-] \tag{18}$$

Short-term behavior of bonded joints under htm-load

Based on the described experimental methods, the following short-term behavior properties of the joints are determined. The results of the tensile tests of adhesively bonded joints, which are saturated at 70 °C and different moisture, are shown in Figure 15. The samples are tested at temperature levels of $\vartheta = 22.5$ °C, $\vartheta = 40$ °C and $\vartheta = 70$ °C.

The strength of the tested specimen shows a strong dependence on the moisture level in the adhesive. The yield point and the fracture strength decrease with increasing moisture. The adhesive is plasticized by water adsorption, resulting in a low strength of the adhesive bond. The plasticizing effect of moisture in the adhesive leads to a reduction of its glass transition temperature T_g [21]. The softening is caused by rupture of the van der Waals bondings and build hydrogen bonds. This effect can be reversed by drying [5]. Of particular importance for the reduction the adhesive strength is the degradation of polymer chains by hydrolysis, which is significantly accelerated by mechanical stress and higher temperature.
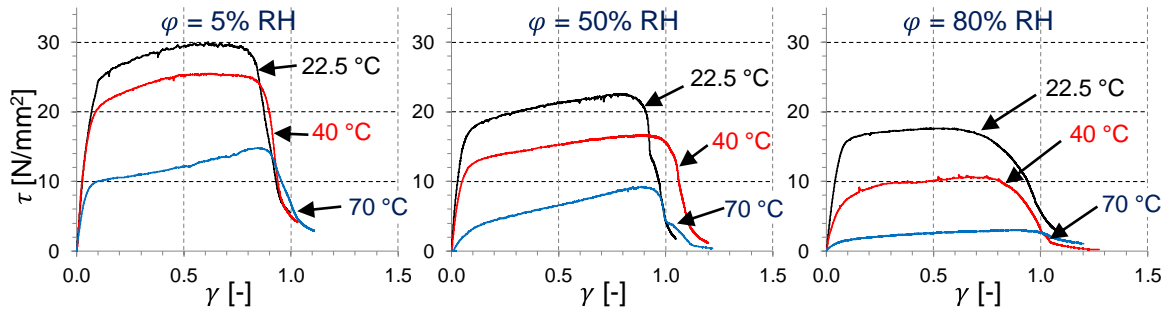
Figure 15: Tensile stress-strain behavior of thick adherends shear specimens (TASS) after

saturation at 70 °C and three different moisture levels tested at different temperature values

The strong influence of the test temperature on the strength is also evident. Higher temperatures in particular lead to the reduction of the adhesive strength. In combination with high moisture concentration, this phenomenon is exacerbated. The yield strength at 70°C - 80% RH is no longer visible, as the adhesive plasticizes strongly. A high water concentration is responsible for lowering the transition point T_g [21], which means that the wet adhesive is closer to the temperature T_g than the dry adhesive at high test temperatures. The absorbed water causes swelling and, thus, internal stresses due to hindered strains by the substrates [23].
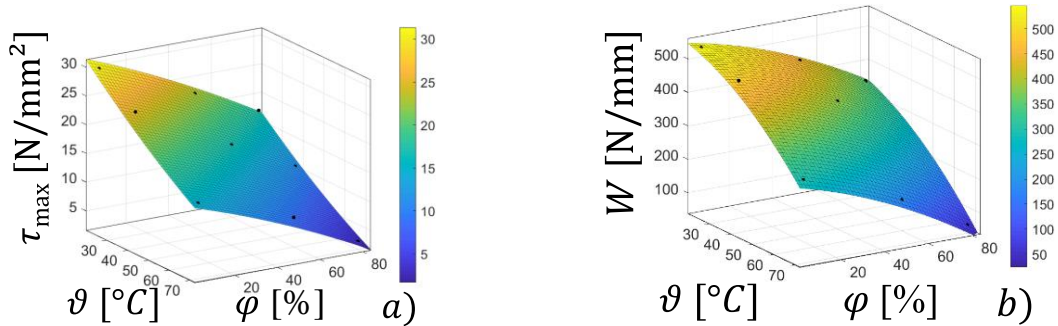

Figure 16: a) *max. shear stress τ_{max} b) energy absorption W of thick adherends shear specimens (TASS) versus temperature and moisture.*

Figure 16 shows further constitutive relationships. It can be seen that the energy absorption W (Figure 16 b)) also depends strongly on temperature and humidity. Both, an increasing humidity as well as temperature strongly reduce the maximum of energy absorption. The shear modulus G and the hardening modulus H were determined by using an extended AVRAMI approach [24].

The shear modulus is also strongly dependent on temperature and humidity. The hardening modulus changes mainly with increasing humidity (*Figure 17*). Changes in the test temperature have no effect on the hardening modulus of the tested TASS.
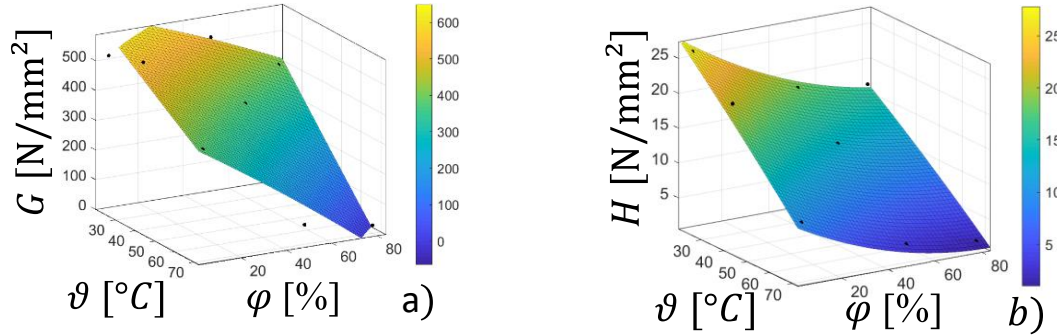

Figure 17: a*) shear modulus G b) hardening modulus H of thick adherends shear specimens (TASS) versus temperature and moisture*.

Conclusion

A methodology for characterizing the water diffusion behavior is presented in order to investigate the influence of moisture on the mechanical properties of a structural epoxy adhesive. The characterization is based on tests, where the adhesive bulk material is exposed to moist air and gains weight over time due to water absorption. The diffusion is characterized by the change in weight. The assumption of one-dimensional diffusion verifies the FE-simulations for the case of thin adhesive specimens.

The assumption of one-dimensional diffusion could be assured by numerical simulation, since the moisture uptake curves of the water diffusion coincide if one- and two-dimensional boundary conditions are applied in the three dimensional analyses. By applying a one-dimensional diffusion model, a thickness of 0.5mm is chosen in order to achieve feasible time intervals for the tests.

For the experimental characterization, the model of Fick's diffusion is chosen, where the diffusion coefficient shows a strong dependence on temperature, while the mass uptake until

saturation mainly depends on the relative humidity of the environment. Basic approaches are applied together with the Fick model of diffusion for the representation of these phenomena. The parameters of the approaches are identified by using the least squares method. The resulting prediction of the water uptake by the Fick model of diffusion is in good agreement with the test data. A model for anomalous, non-FICK diffusion, like the proposed model of the LANGMUIR-type in [4], cf. [6], may show better predictions.

Epoxy adhesives are only hydrolyzed under extreme conditions, in which high relative humidity, temperature and mechanical loading act at the same time. It should be mentioned that hydrolysis only takes place, if a specific activation energy is reached, which is significantly reduced by the influence of the mechanical stress [25]. This is why the mechanical behavior of thick adherends shear specimens (TASS) is investigated together with the hygro-thermal loading. The quasi-static tests show a strong dependence at the mechanical behavior on temperature and humidity. Both, the maximum shear stress as well as the energy absorption of the adhesive decrease strongly with increasing temperature as well as increasing humidity. The hardening modulus changes mainly with rising humidity. Changes in the test temperature have no significant influence on the hardening modulus of the tested TASS. The change in mechanical properties as a function of moisture content and temperature must be taken into account when characterizing adhesives and bonded joints.

Acknowledgements

References

[1]   D. A. Dillard, *Advances in structural adhesive bonding,* in: Woodhead Publishing Series in Welding and Other Joining Technologies, Boca Raton, Fla, Oxford: Woodhead Pub. Ltd, 2010, ISBN: 9781439802175.

[2]   G. Habenicht, *Kleben - Grundlagen, Technologien, Anwendungen*, in: VDI-Buch, 6 th ed., Heidelberg: Springer-Verlag GmbH, 2009, ISBN: 9783540852643.

[3]   A. Lutz, A. Droste and C. Brändli, *Structural bonding in lightweight vehicle construction - Characteristics of modern structural adhesives, simulation and application in bodyshell work and during assembly*, Landsberg: MI Verl. Moderne Industrie, 2013, ISBN: 9783862360666.

[4]   W. Possart and M. Brede, (eds.)., *Adhesive joints, ageing and durability of epoxies and polyurethanes*, Weinheim, Germany: Wiley-VCH, 2019., ISBN: 9783527803750.

[5]   E. M. Petrie, *Epoxy adhesive formulations - Epoxy properties and characteristics; techniques for improving epoxy strength, flexibility, and durability; testing and quality control guidelines*, in: McGraw-Hill chemical engineering, New York, NY: McGraw-Hill, 2006, ISBN: 9780071455442.

[6]   J. Crank, *The mathematics of diffusion,* 2nd ed., Oxford: Clarendon Press, 1976, ISBN: 0198533446.

[7]   A. Ameli, N. V. Datla, M. Papini and J. K. Spelt, *Hygrothermal properties of highly toughened epoxy adhesives*, The Journal of Adhesion, vol. 86, no. 7, page 698–725, 2010, doi: 10.1080/00218464.2010.482405.

[8]   A. Mubashar, I. A. Ashcroft, G. W. Critchlow and A. D. Crocombe, *Moisture absorption–desorption effects in adhesive joints*, International Journal of Adhesion and Adhesives, vol. 29, no. 8, page 751–760, 2009, doi: 10.1016/j.ijadhadh.2009.05.001.

[9]   62:2008, DIN EN ISO 62 *Plastics – Determination of water absorption*, Berlin, 2008.

[10] D. A. Bond and P. A. Smith, *Modeling the transport of low-molecular-weight penetrants within polymer matrix composites*, Applied Mechanics Reviews, vol. 59, no. 5, page 249–268, 2006, doi: 10.1115/1.2202873.

[11] W. Jost, *Diffusion in solids, liquids, gases,* in: Physical chemistry, vol. 1, 3rd ed., New York: Acad. Press, 1969, ISBN: 0-12-390750-0.

[12] H. Twardy, *Wasserdampfdifussion in CFK-Messung des Diffusionskoeffizienten bei Konzentrationsabhängigkeit*, Wiss. Berichtswesen d. DFVLR, 1984.

[13] A. Fick, *Ueber Diffusion*, Ann. Phys. Chem., vol. 170, no. 1, page 59–86, 1855, doi: 10.1002/andp.18551700105.

[14] H. Mehrer, *Diffusion in Solids - Fundamentals, Methods, Materials, Diffusion-Controlled Processes*, in: Springer Series in Solid-State Sciences, vol. 155, Heidelberg: Springer-Verlag GmbH, 2007, ISBN: 9783540714866.

[15] C. Bieker, *Methodenentwicklung zur Bestimmung des hygrothermomechanischen Langzeitverhaltens von strukturellen Klebverbindungen mit metallischen und mineralischen Untergründen*, Diss. at University Kassel, 2006, in: Schriftenreihe des Instituts für Werkstofftechnik Kassel: Shaker Verlag, Aachen 2006, ISBN: 3-8322-5433-1.

[16] DYNA, *LS-DYNA keyword user's manual*, Version 971 R7, Livermore Software Technology Corporation, Livermore, CA, 2014. Available at https://www.dynasupport.com/manuals.

[17] S. Yoon, B. Han and Z. Wang, *On moisture diffusion modeling using thermal-moisture analogy*, Journal of Electronic Packaging, vol. 129, no. 4, page 421–426, 2007, doi: 10.1115/1.2804090.

[18] S. Sander, U. Kroll, G. Meschut and A. Matzenmiller, *Methodenentwicklung zur Langzeitprognose von Klebverbindungen bei kombinierter Temperatur- und Medieneinwirkung*, to be published in: Schriftenreihe Forschung für die Praxis P 1243,

Im Stahlzentrum, Verlag- und Vertriebsgesellschaft mbH, Sohnstr. 65 Düsseldorf, 2020.

[19]   Y. C. Lin and X. Chen, *Moisture sorption–desorption–resorption characteristics and its effect on the mechanical behavior of the epoxy system*, Polymer, vol. 46, no. 25, page 11994–12003, 2005, doi: 10.1016/j.polymer.2005.10.002.

[20]   S. Sugiman, A. D. Crocombe and I. A. Aschroft, *Experimental and numerical investigation of the static response of environmentally aged adhesively bonded joints*, International Journal of Adhesion and Adhesives, vol. 40, page 224–237, 2013, doi: 10.1016/j.ijadhadh.2012.08.007.

[21]   G. Viana, M. Costa, M. D. Banea and L. F. M. da Silva, *Behaviour of environmentally degraded epoxy adhesives as a function of temperature*, The Journal of Adhesion, vol. 93, no. 1-2, page 95–112, 2017, doi: 10.1080/00218464.2016.1179118.

[22]   G. Viana, M. Costa, M. D. Banea and L. F. da Silva, *A review on the temperature and moisture degradation of adhesive joints*, Proceedings of the Institution of Mechanical Engineers, vol. 231, no. 5, page 488–501, 2017, doi: 10.1177/1464420716671503.

[23]   C. Liljedahl, A. D. Crocombe, F. E. Gauntlett, M. S. Rihawy and A. S. Clough, *Characterising moisture ingress in adhesively bonded joints using nuclear reaction analysis*, International Journal of Adhesion and Adhesives, vol. 29, no. 4, page 356–360, 2009, doi: 10.1016/j.ijadhadh.2008.07.005.

[24]   M. Schlimmer and C. Barthel, *Systematische Ermittlung von Kennwerten*, adhäsion, vol. 55, no. 3, page 28–32, 2011, doi: 10.1365/s35145-011-0013-2.

[25]   J. Comyn, *Adhesion Science,* in: RSC Paperbacks, vol.12: Royal Society of Chemistry, Cambridge 1997, ISBN: 978-0-85404-543-3.